Journal of Physical and Theoretical Chemistry
of Islamic Azad University of Iran, 8 (4) 317-327: Winter 2012
(J. Phys. Theor. Chem. IAU Iran)
ISSN 1735-2126

Modeling Investigation of Dielectric Constant Effect on NMR and IR Properties of C48 as a Single Walled Carbon Nanotube

S. M. Sadat Choobeh [1] and F. Mollaamin[2*]

[1] M.Sc. Student, Science and Research Branch, Islamic Azad University, Tehran, Iran
[2] Department of Chemistry, Qom Branch, Islamic Azad University, Qom, Iran

Received March 2012; Accepted April 2012

ABSTRACT

A cluster model for active site of nanotube (C48) was presented and investigated the geometric structure and thermochemical parameters. Quantum-mechanical calculations were performed at the HF / STO-3G, 6-31G, 6-31G* and 6-31G** levels of theory in the gas phase and three solvents at four temperatures. Also, nuclear shielding parameters of the active site of nanotube have been taken into account using GIAO method at the HF / STO-3G,6-31G,6-31G* and 6-31G** levels of theory in the gas phase and in different solvents such as water, methanol, ethanol. The results were revealed that the NMR chemical shielding parameters are strongly affected by inducing different solvent media. According to these theoretical results of energy values, some important relationships have been found between the dielectric constant and structural stability of active site of nanotube.

Keywords: Carbon nanotube; Modeling; NMR; IR; DFT; Solvent

INTRODUCTION

The discovery of carbon nanotubes in the soot produced by an arc-discharge of graphite, first reported by Iijima in 1991 [1], has ushered in a new, and very active, research field in theoretical and experimental condensed matter physics, and materials science, world-wide[2]. Carbon nanotubes are sheets of graphite that has been rolled into a tube [3]. Most important structures are single walled nanotubes (SWCNTs) and multi walled nanotubes (MWCNTs). Carbon nanotubes are quasi one-dimensional systems: the atoms are located on a cylindrical surface in three-dimensional space. SWCNTs are made of a single seamlessly rolled graphite sheet with a typical diameter of about 1.4 nm which is similar to a buckyball (C60). In the case of SWCNTs, the diameters typically range from 0.4 to 2 nm, and lengths up to 1.5 cm have been reported [4].Such dimensions induce very high aspect ratios (length/diameter – over 10 million) [5] have given a detailed description of the nanotube structure [6]. They may be used as molecular field-effect transistors [7,8], electron field emitters [7,9], artificial muscles [7,10] or even DNA sequencing agents [11]. Individual classes of tubes might exhibit variety of different physical and chemical properties [12]. The physics of carbon nanotubes is intimately bound up with the emerging and exciting fields of computational nano - science, computational

* Corresponding author: smollaamin@gmail.com

nano - technology, computational materials science and computational condensed matter physics. Nano-science and nano-technology are all based on two pillars; numerical modeling and computer-based simulation, to compute the mechanical, thermal and electronic properties of nano-scale structures, and nano-scale processes that unfolding nanoscopic systems. Computational nano-science forms an indispensable pathway in the research concerned with the purposeful manipulation and structural transformation of condensed phases at their most fundamental levels. This field of research allows us to exercise a complete control over the structure and functioning of physical matter at the atomistic and molecular scales. Computational predictive nano-scale modeling offers an invaluable tool for the design, fabrication, and quality control of devices and components that will form the constituents of nano-technology and molecular engineering [2]. Functionalization of single walled carbon nanotubes (SWNTs), which means modifying the physical and chemical properties of SWNTs by adsorption of foreign atoms and molecules, carries great potential in tailoring new nanostructures for desired applications [13] of SWNT by attaching various molecules or molecular complexes to its exterior wall or tips [14],or by stuffing smaller nanoparticles/molecules into its hollow interior [15,16] has been extensively studied due to its potential in facilitating miniature nanodevices and nanocircuits for broad applications. From previous studies, it was shown that the mechanical, electronic and magnetic properties of SWNT can be drastically changed by both physical and chemical adsorption of foreign atoms and molecules [17].

COMPUTATIONAL METHODS

The edifice of computational nano-science is based on two foundations; one, the use of highly advanced many-body quantum mechanical-based concepts and methods, such as the density functional theory (DFT) of atoms and molecules, for an ab initio investigation of nano-systems composed of several ten to several hundred atoms; two, the use of highly advanced classical statistical mechanics-based models and methods, such as the molecular dynamics (MD) simulation method, for modeling nano-scale structures and processes composed of several thousand to several million atoms. [2].

The semi empirical studies are based on a fourth moment tight binding approximation combined with canonical the Monte Carlo (MC) [18,19].This method complements the DFT calculations since it allows simulations at finite temperatures with good statistics [20].

The term “ab initio” is given to computations that are derived directly from theoretical principles, with no inclusion of experimental data. The most common type of ab initio calculation is a Hartree Fock calculation (HF), in which the primary approximation is called the central field approximation. A method that avoids making the HF mistakes is called Quantum Monte Carlo (QMC). There are several flavors of QMC: variation, diffusion and Green’s functions. These methods work with an explicitly correlated wave function and evaluate integrals numerically using a Monte Carlo integration. These calculations can be time consuming, but they are probably the most accurate methods known today. In general, ab initio calculations provide good qualitative results and can give increasingly accurate quantitative results as the molecules in question become smaller [21].

In this study, difference in force field is illustrated by comparing the energy calculated by using force fields, The quantum mechanics (QM) calculations were carried out with theGAUSSIAN98 program based on HF/sto-3G& HF/6-31G& HF/6-31G*& HF/-31G**levels. In the Gaussian program a simple approximation is used in which the volume of the solute is used to compute the

radius of a cavity which forms the hypothetical surface of the molecule [22,23]. Then we have compared gas phase and different solvent media such as water, methanol, ethanol, and mixtures of them. So, we investigated polar solvent effects on SWCNT within the Onsager self-consistent reaction field (SCRF) model using a Hartree-Fock method and the temperature effects (between 294K and 302K) on the stability of SWCNT in various solvents.

In this investigation, charge distribution, geometry optimizations and thermodynamic properties were employed with different model chemistries (sto-3g, 6-31g, 6-31g* and 6-31g**) in various solvents (water, ethanol and methanol) at diverse temperatures (294,296,300,302). The most popular self-consistent reaction field (SCRF) methods, based on apparent surface charges, is named as PCM, which has been extended to deal with nonelectrostatic effects using scaled particle theory, as formulated by Pierotti and modified subsequently in[24,25] .

Data collected at 294,296,300 and 302K were analyzed to obtain the thermodynamic parameters ΔG, ΔH and ΔS. Also electromotive force (E) has been calculated from Gibbs free energy, while ΔS was calculated from the following relationship:

$$\Delta G = \Delta H - T\Delta S \quad (1)$$

The equilibrium free energy of solvation can be divided into smaller contributions corresponding to cavitation; universal solvation effect such as solute-solvent electrostatic, dispersion and repulsion interactions, and no universal specific interaction, such as intermolecular hydrogen bonding or electron donor-electron acceptor interactions [26]:

$$\Delta G(\text{solvation}) = \Delta G(\text{electrostatic}) + \Delta G(\text{dispersion}) + \Delta G(\text{repulsion}) + \Delta G(\text{cavitation}) + \Delta G(\text{specific}). \quad (2)$$

We have presented a comparison of ΔG, ΔH, ΔS and E derived from these data, including vinblastine solvent, which is entropically driven via water, methanol and ethanol release.

The calculations were performed at different levels of theory to obtain the more accurate equilibrium geometrical parameters and IR spectral data for each of the determined structure. It is assumed that including additional diffuse and polarization functions into the basis set used in the calculation always leads to considerable improvements on the obtained results in theory [27]. The electronic structure plays a primary role in determining structure of a molecule. However, changes of the electronic energy associated with a chemical process are comparable, in many cases, with those owed to solvation in solution. The coupling of continuum models with quantum chemical calculations using SCRF approaches [28,29].has been implemented over the past decade in a number of widely available ab initio quantum chemistry program such as Gaussian 98. To test the influence of the polarized continuum on molecular structure the geometry optimizations were also made in water, methanol and ethanol using self-consistent reaction field (SCRF = dipole) which uses a more reliable cavity as union of a series of interlocking atomic spheres. Over the past decades the NMR chemical shift measurement in solutions has been applied to a vast range of problems in chemistry and biochemistry and has revealed itself to be an invaluable microscopic probe. It has played an especially important role in the structural understanding of protein owing to its great sensitivity to the environment in which the probing atom is situated. Theories of the chemical shift in solution, on the other hand, have not been well developed owing to the lack of a theory for describing the electronic structure of a solvated molecule.

The gauge including atomic orbitals (GIAO) or applying a “continuous set of gauge transformations (CSGT) are adopted to solve the gauge problem in the calculation of nuclear magnetic shielding [30].

The study of chemical shift reveals a serious drawback inherent in the classical–quantum hybrid approach. The solvent effects on the chemical shift showed temperature dependence opposite to corresponding experimental results. An ab initio analysis suggested strongly that the ill behavior is originated from the lack of electron exchange between solute and solvent. The computations refer to vinblastine molecule, unpolarized by any solvent molecules, whereas the NMR shift measurements were made in water, methanol and ethanol (78.39, 32.63 and 24.55, respectively) [30-34].

Ab initio calculation of nuclear magnetic shielding has become an indispensable aid in the analysis of molecular structure and accurate assignment of NMR spectra of compounds [31].NMR is based on the quantum mechanical property of nuclei. The chemical shielding refers to the phenomenon, which associated with the secondary magnetic field created by the induced motions of the electrons that surrounding the nuclei when in the presence of an applied magnetic field. For chemical shielding (CS) tensor, which describes how the size of shielding varies with molecular orientation, we recurrently use the following convention for the three principle component:

$$\sigma_{11} \leq \sigma_{22} \leq \sigma_{33} \quad (3)$$

The three values of the shielding tensor are frequently expressed as the isotropic value (σ_{iso}), anisotropy shielding ($\Delta\sigma$) and asymmetry parameter (η). Calculations of nucleus-dependent and -independent chemical shifts were carried out using the gauge-invariant atomic orbital (GIAO) approach. The magnetic susceptibility was computed using continuous set gauge transformation (CSGT) methods. The energy of solvation can be divided into terms that explain the bulk solvent and terms that specify the first solvation shell. The bulk solvent contribution is principally the result of dielectric shielding of electrostatic charge interactions. In the simplest form, it can be included in electrostatic interactions by means of the dielectric constant ε, as in the Coulomb interaction equation [35-37].

$$\varepsilon = q_i q_j / \varepsilon r_{ij} \quad (4)$$

RESULTS AND DISCUSSION

In this work, we studied the structural properties and adsorption of water, methanol and ethanol surrounding SWCNTs using molecular dynamics simulations. At first, we have modeled the nanotube in different solvent with HyperChem 7 package. The optimized structures of nanotubes in different media are shown in scheme 1. We used different force fields to determine energy and other type of geometrical parameters on the particular SWCNT.

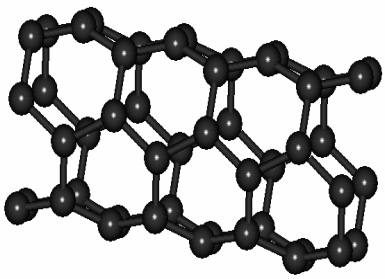

a) C_{48} (3,3)

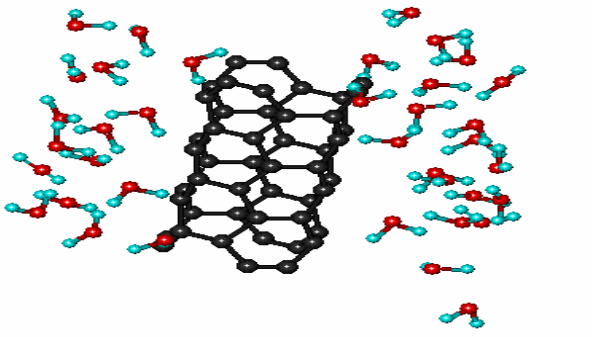

b) C_{48} (3,3)-water

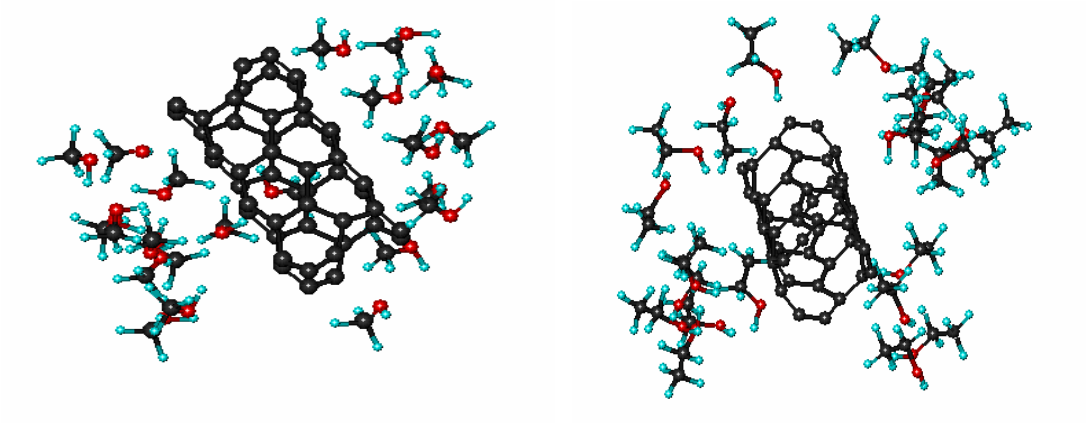

c) C_{48} (3,3)- methanol **d)** C_{48} (3,3)-ethanol

Scheme 1. Optimized structure of nanotube in different media.

The calculations of the relative harmonic frequencies, IR intensities and ΔH, ΔG, ΔS for active points of vinblastine are presented in Table1. ΔH, ΔG (kcal mol^{-1}) and ΔS (cal $mol^{-1}K^{-1}$) indicate the consistency at different temperatures as is shown in Figure 1 (a),(b),(c) and (d) the variation of Gibbs free energy behave in the same way in water, methanol and ethanol solvents at HF levels, respectively. As it is obvious in Fig.1(a),(b),(c) and (d), these parameters are obtained by the relation coefficients R^2=1(Fig.1 a) for STO_3G and R^2=1.001 (Fig.1b) for 6-31G and R^2=0.999(Fig.1c) for 6-31G* and R^2=1 (Fig.1d) for 6-31G** and equations as follows:

$\Delta G = 10^{-6} - 0.129T$ (a)
$\Delta G = 10^{-6} - 0.133T$ (b)
$\Delta G = 10^{-6} - 0.138T$ (c)
$\Delta G = 10^{-6} - 0.14T$ (d)

In Fig. 1., we have observed that by increasing temperature, ΔG is decreased. In this study, the high level of Gibbs free energy and electromotive force correlation and significance (R^2) for all these compounds indicate that similar processes are involved regardless of the nature of their chemical environment. Note that the slope of the ΔH–ΔS or the compensation temperature is different from the mean temperature over which the parameters were estimated.

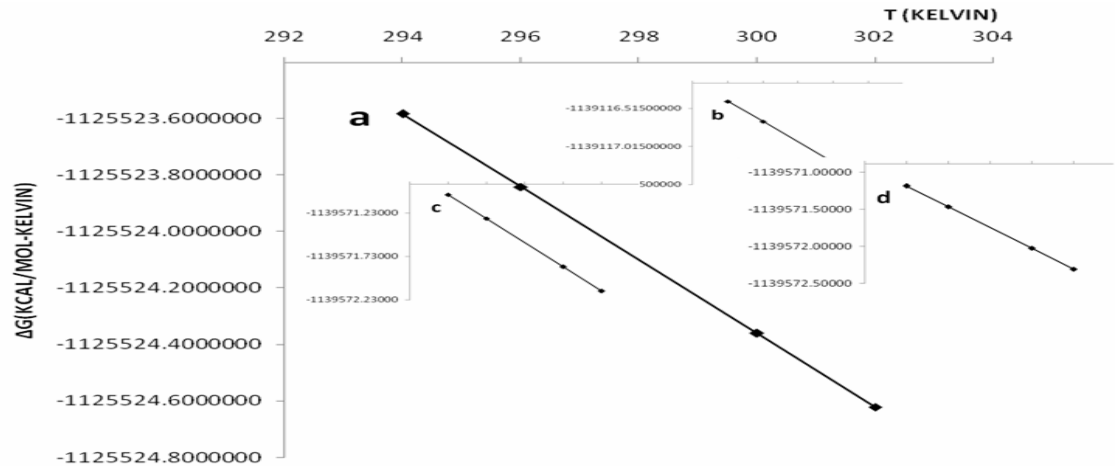

Fig.1. Calculated ΔG in various basis sets **a)** STO_3G ,**b)** 6-31G,**c)** 6-31g* ,**d)** 6-31g** at different temperature (water, ethanol and methanol).

Table 1. Thermodynamic parameters at different temperature using different methods

Basis set	Temp.	E (KCAL/MOL-KELVIN)	H (KCAL/MOL-KELVIN)	G (KCAL/MOL-KELVIN)	ΔS (CAL/MOL-KELVIN)
Sto-3G	294	-1125486.39015	-1125485.80595	-1125523.58333	128.497
	296	-1125486.20064	-1125485.61268	-1125523.84123	129.152
	300	-1125485.81787	-1125485.22174	-1125524.36017	130.464
	302	-1125485.62397	-1125485.02408	-1125524.62184	131.121
6-31G	294	-1139078.09411	-1139077.50991	-1139116.42370	132.362
	296	-1139077.89520	-1139077.30723	-1139116.68913	133.049
	300	-1139077.49297	-1139076.89684	-1139117.22439	134.426
	302	-1139077.28966	-1139076.68914	-1139117.49358	135.115
6-31G*	294	-1139531.20371	-1139530.61950	-1139571.01921	137.417
	296	-1139531.00165	-1139530.41368	-1139571.29468	138.115
	300	-1139530.59315	-1139529.99702	-1139571.85002	139.512
	302	-1139530.38670	-1139529.78681	-1139572.12988	140.211
6-31G**	294	-1139531.00730	-1139530.42310	-1139571.18675	138.653
	296	-1139530.80587	-1139530.21790	-1139571.46473	139.350
	300	-1139530.39862	-1139529.80250	-1139572.02509	140.745
	302	-1139530.19218	-1139529.59229	-1139572.30684	141.442

NMR calculations on vinblastine using Hartree-Fock (HF) and density functional theory (DFT) reveal that methods including electron correlation show significant improvements in the NMR shielding over results. It might be suggested that optimization of solute molecule in solvent followed by shielding calculations is similar to shielding calculations of solvent ± solute system. However, if the molecule is first optimized in gas phase and then NMR shielding calculations is performed in the solvent, the solvent ± solute interactions are taken into consideration for NMR shielding calculation.

Therefore in solvent effect studies, it is more advisable to carry out shielding calculations in solution even with a fixed (gas and solvent-phase optimized) solute geometry, than to perform shielding computations in vacuum for a solute where the geometry is optimized in solution.

The NMR measurements were carried out using HF, /sto-3g,6-31g,6-31g*,6-31g** in GIAO method of nuclear magnetic resonance at theoretical concepts in different dielectric constants(gas, water, methanol and ethanol) (Tables 2). The results of Tables 2 are shown in Figs 2, 3 and 4, where we plot the chemical shift (δ) and chemical shift anisotropy (Δσ) of the vinblastine for each active atoms (C1-C12). We have found that C8 in gas, C6 in solvent phase denoted has maximal shift and other indicated atoms almost have the similar shifts in different positions. Also, we have seen that by increasing dielectric constant, value of chemical shift and chemical anisotropy has been increased. In Figure5, we have observed that total energy of methanol is less than others so it can be the better solvent for this research.

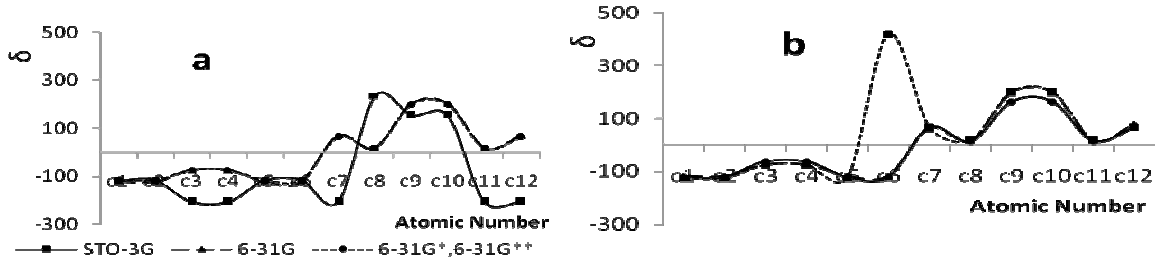

Fig. 2. Comparing of δ shielding values at the HF, level with the STO-3G, 6-31G, 6-31G*, 6-31G** basis sets in GIAO method between **a)** gas and b**)** solvent phases.

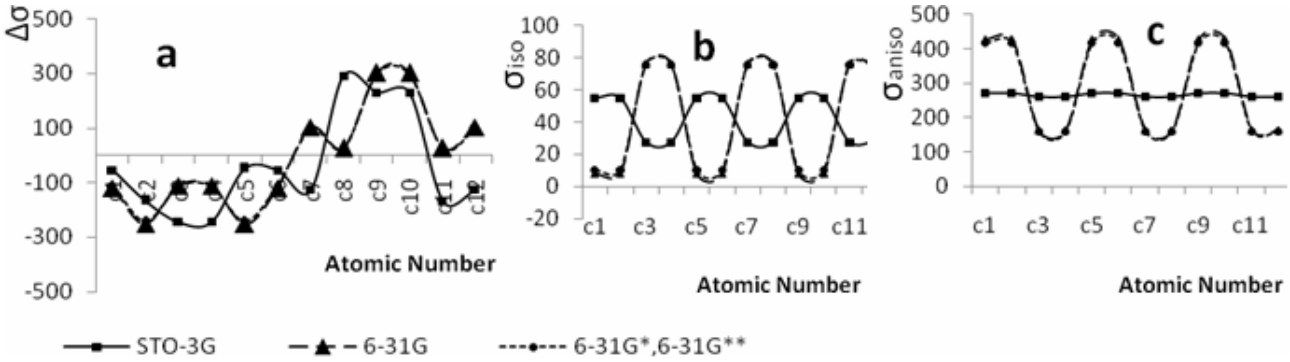

Fig. 3. The graphs of **a)** Δσ shielding values ,**b)** isotropic shielding values(σ_{iso}), c**)** anisotropic shielding values (σ_{aniso}), of propose atoms of nanotube in gas phases at the HF, level with the STO-3G, 6-31G ,6-31G*,6-31G** basis sets in GIAO method.

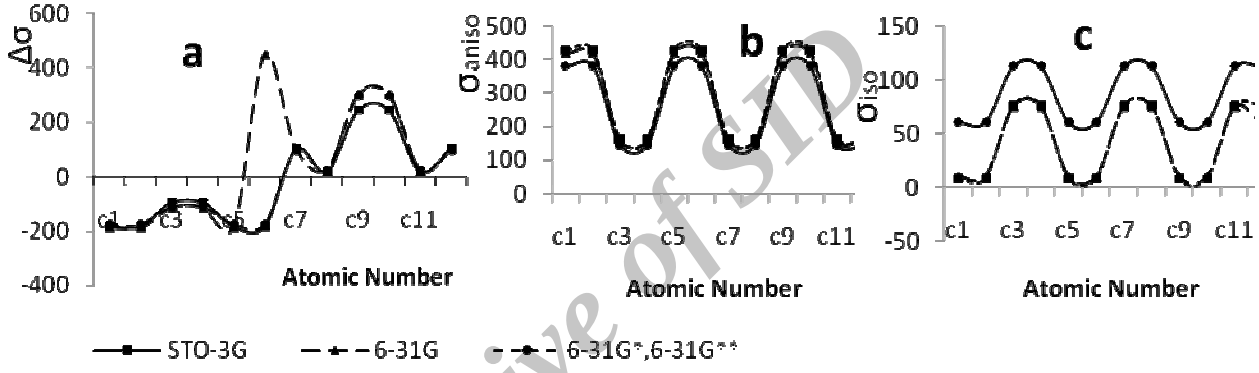

Fig. 4. The graphs of **a)** Δσ shielding values ,**b)** isotropic shielding values(σ_{iso}), **c)** anisotropic shielding values(σ_{aniso}), of propose atoms of nanotube in solvent phases at the HF, level with the STO-3G, 6-31G ,6-31G*,6-31G** basis sets in GIAO method.

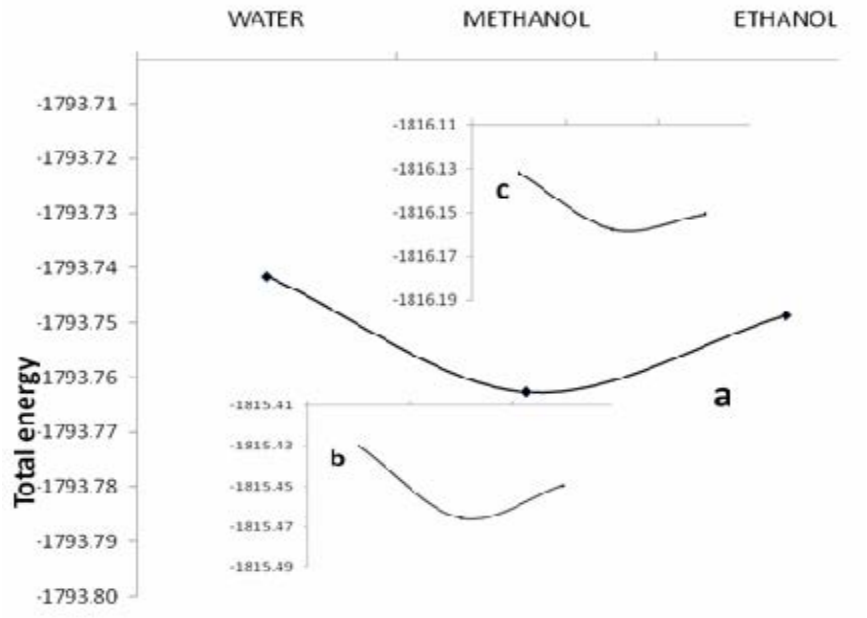

Fig. 5. Total energy in various dielectric constants (water, methanol and ethanol).

Table 2. NMR Properties of C48 in different dielectric constants at the HF level with the STO-3G, 6-31G, 6-31G*, 6-31G** basis sets in GIAO method

gas												
basis set	NO.C	Δσ	η	δ	σ11-iso	σ33-iso	basis set	NO.C	Δσ	η	δ	σ11-iso	σ33-iso
Sto-3G	1	-55.4062	0.146156	-119.019	68.2072	-119.019	6-31G*	1	-110.99	-0.09394	-115.819	52.4694	-115.819
	2	-166.494	-1.72057	-119.019	-42.8809	-119.019		2	-240.533	-2.33093	-115.819	-77.073	-115.819
	3	-243.831	-0.62028	-207.287	39.3551	-207.287		3	-112.626	-1.10971	-75.0839	-75.0839	-4.1188
	4	-243.831	-0.62028	-207.287	39.3551	-207.287		4	-112.626	-1.10971	-75.0839	-75.0839	-4.1188
	5	-49.1561	0.251183	-119.019	-42.8809	-119.019		5	-240.533	-2.33093	-115.819	-77.073	-115.819
	6	-55.4062	0.146156	-119.019	68.2072	-119.019		6	-110.99	-0.09394	-115.819	52.4694	-115.819
	7	-126.226	0.51443	-207.287	156.9605	-207.287		7	96.01645	-0.87131	64.011	64.011	-4.1188
	8	290.2872	1.287488	232.9801	232.9801	-207.287		8	25.8769	-0.52249	17.2513	17.2513	-4.1188
	9	229.8035	0.55375	153.2023	153.2023	-119.019		9	297.4972	0.167929	198.3315	198.3315	-115.819
	10	229.8035	0.55375	153.2023	153.2023	-119.019		10	297.4972	0.167929	198.3315	198.3315	-115.819
	11	-168.572	0.105852	-207.287	114.6141	-207.287		11	25.8769	-0.52249	17.2513	17.2513	-4.1188
	12	-126.226	0.51443	-207.287	156.9605	-207.287		12	96.01645	-0.87131	64.011	64.011	-4.1188
6-31G	1	-120.143	-0.06835	-123.918	57.7244	-123.918	6-31G**	1	-110.99	-0.09394	-115.819	52.4694	-115.819
	2	-251.334	-2.18572	-123.918	-73.4662	-123.918		2	-240.533	-2.33093	-115.819	-77.073	-115.819
	3	-111.606	-1.22289	-74.4039	-74.4039	-8.2919		3	-112.626	-1.10971	-75.0839	-75.0839	-4.1188
	4	-111.606	-1.22289	-74.4039	-74.4039	-8.2919		4	-112.626	-1.10971	-75.0839	-75.0839	-4.1188
	5	-251.334	-2.18572	-123.918	-73.4662	-123.918		5	-240.533	-2.33093	-115.819	-77.073	-115.819
	6	-120.143	-0.06835	-123.918	57.7244	-123.918		6	-110.99	-0.09394	-115.819	52.4694	-115.819
	7	103.3999	-0.75942	68.9333	68.9333	-8.2919		7	96.01645	-0.87131	64.011	64.011	-4.1188
	8	26.863	-0.07398	17.9087	17.9087	-8.2919		8	25.8769	-0.52249	17.2513	17.2513	-4.1188
	9	302.4287	0.229231	201.6191	201.6191	-123.918		9	297.4972	0.167929	198.3315	198.3315	-115.819
	10	302.4287	0.229231	201.6191	201.6191	-123.918		10	297.4972	0.167929	198.3315	198.3315	-115.819
	11	26.863	-0.07398	17.9087	17.9087	-8.2919		11	25.8769	-0.52249	17.2513	17.2513	-4.1188
	12	103.3999	-0.75942	68.9333	68.9333	-8.2919		12	96.01645	-0.87131	64.011	64.011	-4.1188

Continue Table 2

solvent												
basis set	NO.C	Δσ	η	δ	σ11-iso	σ33-iso	basis set	NO.C	Δσ	η	δ	σ11-iso	σ33-iso
Sto-3G	1	-182.351	-1.52711	-121.567	57.4882	-121.567	6-31G*	1	-174.7	-1.54498	-116.466	52.995	-116.466
	2	-182.351	-2.32023	-121.567	-38.9291	-121.567		2	-174.7	-2.66422	-116.466	-77.3585	-116.466
	3	-94.333	-1.3916	-62.8886	-62.8886	-12.3134		3	-112.492	-1.11282	-74.9945	-74.9945	-4.2307
	4	-94.333	-1.3916	-62.8886	-62.8886	-12.3134		4	-112.492	-1.11282	-74.9945	-74.9945	-4.2307
	5	-182.351	-2.32023	-121.567	-38.9291	-121.567		5	-174.7	-2.66422	-116.466	-77.3585	-116.466
	6	-182.351	-1.52711	-121.567	57.4882	-121.567		6	-174.7	-1.54498	-116.466	52.995	-116.466
	7	102.0652	-0.63807	68.0435	68.0435	-12.3134		7	96.23795	-0.86812	64.1586	64.1586	-4.2307
	8	19.9729	0.849519	13.3153	13.3153	-12.3134		8	25.77275	-0.50754	17.1818	17.1818	-4.2307
	9	245.6879	0.484413	163.7919	163.7919	-121.567		9	298.5948	0.170144	199.0632	199.0632	-116.466
	10	245.6879	0.484413	163.7919	163.7919	-121.567		10	298.5948	0.170144	199.0632	199.0632	-116.466
	11	19.9729	0.849519	13.3153	13.3153	-12.3134		11	25.77275	-0.50754	17.1818	17.1818	-4.2307
	12	102.0652	-0.63807	68.0435	68.0435	-12.3134		12	96.23795	-0.86812	64.1586	64.1586	-4.2307
6-31G	1	-185.748	-1.53274	-123.832	57.8616	-123.832	6-31G**	1	-174.7	-1.54498	-116.466	52.995	-116.466
	2	-185.748	-2.59558	-123.832	-73.7514	-123.832		2	-174.7	-2.66422	-116.466	-77.3585	-116.466
	3	-111.829	-1.21639	-74.5524	-74.5524	-8.0663		3	-112.492	-1.11282	-74.9945	-74.9945	-4.2307
	4	-111.829	-1.21639	-74.5524	-74.5524	-8.0663		4	-112.492	-1.11282	-74.9945	-74.9945	-4.2307
	5	-185.748	-2.59558	-123.832	-73.7514	-123.832		5	-174.7	-2.66422	-116.466	-77.3585	-116.466
	6	-185.748	-1.53274	-123.832	57.8616	-123.832		6	-174.7	-1.54498	-116.466	52.995	-116.466
	7	103.2445	-0.76562	68.8296	68.8296	-8.0663		7	96.23795	-0.86812	64.1586	64.1586	-4.2307
	8	26.7332	-0.0948	17.8221	17.8221	-8.0663		8	25.77275	-0.50754	17.1818	17.1818	-4.2307
	9	302.4564	0.228261	201.6376	201.6376	-123.832		9	298.5948	0.170144	199.0632	199.0632	-116.466
	10	302.4564	0.228261	201.6376	201.6376	-123.832		10	298.5948	0.170144	199.0632	199.0632	-116.466
	11	26.7332	-0.0948	17.8221	17.8221	-8.0663		11	25.77275	-0.50754	17.1818	17.1818	-4.2307
	12	103.2445	-0.76562	68.8296	68.8296	-8.0663		12	96.23795	-0.86812	64.1586	64.1586	-4.2307

CONCLUSION

In this work, we investigated the effects of polar solvents and different temperatures on the stability of SWCNT in various solvents. Ab initio calculations were carried out with GAUSSIAN 98 program at the HF/STO-3G and 6-31G and 6-31G* and 6-31G**level of theory. The results obtained from Onsager model calculations are illustrated using the energy difference between these conformers which are quite sensitive to the polarity of the surrounding solvent, that the methanol solvent can be suggested as the most compatible solvent for studying the structural properties of SWCNT.

ΔS and ΔH values increase with temperatures but ΔG decreases; but the variations of solvent and temperature have a considerable effect on ΔS.

To conclude, we have performed simulations and solvent NMR of theoretical methodology on vinblastine at constant fields and temperatures 294-302 K by various solvent constants.

Our calculations have demonstrated that such extrapolation schemes significantly overestimate the vinblastine-to-gas and solvent phases shifts that the 8 and 6 were the most active point at indicated structure.

REFERENCES

[1] S. Iijima, Nature (London), 354 (1991) 56.

[2] H Rafii-Tabar, Physics Reports, 390 (2004) 235.

[3] E. Thostenson, Z. Ren, T. Chou, a review.Comp. Sci. Technol 61(13) (2001) 1899.

[4] S. Huang, M. Woodson, R. Smalley, J. Liu, Nano Lett., 4 (2004) 1025.

[5] T. Belin, F. Epron. Materials Science and Engineering B, 119 (2005)105.

[6] S. Wijewardane, A review article. Solar Energy, 83 (2009) 1379.

[7] A. Minett, K. Atkinson, S. Roth, CarbonNanotubes. in Handbook of Porous Solids. Edited by Sch üth F, Sing SW, Weitkamp J: Wiley-VCH, Weinheim; 2002.

[8] Z. Yao, H. WC. Postma, L. Balents, C. Dekker, Nature 402 (1999) 273.

[9] O. Zhou, H. Shimoda, B. Gao, S. Oh, L. Fleming, G. Yue, Acc.Chem.Res, 35 (2002) 1045.

[10] R. H. Baughman, C. Cui, A. A. Zakhidov, Z. Iqbal, J. N. Barisci, G. M. Spinks, G. G. Wallace, A. Mazzoldi, D. De Rossi, A. G. Rinzler, O. Jaschinski, S. Roth, M. Kertesz, Science, 284 (1999), 1340.

[11] H. Gao, Y. Kong, D. Cui, Nano Lett., 3 (2003) 471.

[12] M. Monajjemi, V. S. Lee, M. Khaleghian, B. Honarparvar, F. Mollaamin, J. Phys. Chem. C, 114 (2010) 15315.

[13] S. Ciraci, S. Dag, T. Yildirim, O. Gülseren, R. T. Senger, J. Phys.: Condens, 16 (2004) R901.

[14] M. Zhao, Y. Xia, J. P. Lewis, L Mei, J. Phys. Chem. B, 108 (2004) 4711.

[15] B. Huang, Y. Xia, M. Zhao, F. Li, X. Liu , Y. Ji, C. Song, J. Chem. Phys, 122 (2004) 084708.

[16] Y. J. Kang, J. Choi, C. Y. Moon, K. J. Chang, Phys. Rev. B, 71 (2005) 115441.

[17] C. Song, Y. Xia, M. Zhao, X. Liu, F. Li, B. Huang, Chemical Physics Letters, 415 (2005) 183.

[18] H. Amara, J. M. Roussel, C. Bichara, J. P. Gaspard, Phys Rev B, 79 (1) (2009) 014109.

[19] D. Frenkel, B. Smit: Molecular simulation: from algorithms to applications. London, UK: Oxford University Press; 1997.

[20] W. Zhu, A. Börjesson, K. Bolton, Carbon, 48 (2010) 470.

[21] M. Khaleghian, M. Zahmatkesh, F. Mollaamin, M. Monajjemi, Fullerenes, Nanotubes and Carbon Nanostructures; 2010.
[22] E. Westhof, D. L. Beveridge, Hydration of Nucleic Acids. Water Science Reviews, edited by Francs F: Cambridge University Press, New York; 1989.
[23] X. C. Wang, J. Nichols, M. Feyereisen, M. Gutovski, J. Boatz, A. D. J. Haymet, J. Simons, J. Phys. Chem., 95 (1991) 10419.
[24] G. Cohen, H. Eisenberg, Biopolymers, 6 (1968) 1077.
[25] P. Beak, J. B. Covington, S. G. Smith, J. M. White, J. M. Zeiger, J. Org. Chem, 45 (1980) 1354.
[26] P. V. R. Schleyer, Encyclopedia of Computational Chemistry. Chichester: Wiley; 4:2547, 1998.
[27] F. Mollaamin, Z. Varmaghani , M. Monajjemi, Physics and Chemistry of Liquids, 49, (2011), 318.
[28] D. J. Tannor, B. Marten, R. Murphy, R. A. Friesner, D. Sitkoff, A. Nicholls, M. Ring, W. Nalda, A. God-dard, B. Honig, J. Am. Chem. Soc., 116 (1994) 11875.
[29] J. Tomasi, M. Persico, Chem. Rev., 94 (1994) 2027.
[30] M. Monajjemi, L. Saedi, F. Najafi, F. Mollaamin, International Journal of the Physical Sciences, 5 (2010) 1609.
[31] M. Monajjemi, M. Heshmat, H. Aghaei, R. Ahmadi, K. Zare, Bull. Chem. Soc. Ethiopia, 21 (2007) 111.
[32] M. Monajjemi, L. Mahdavian, F. Mollaamin, Bull. Chem. Soc. Ethiop, 22 (2008) 1.
[33] M. Monajjemi, E. Rajaeian, F. Mollamin, F. Naderi, S. Saki, Phys. Chem. Liquids, 46 (2008) 299.
[34] M. Monajjemi, M. H. Razavian, F. Mollaamin, F. Naderi, B. Honarparvar, Russian J. Phys. Chem., 82 (2008) 113.
[35] D. C. Young, Solvation Computational Chemistry: A Practical Guide for Applying Techniques to Real-World Problems. Wiley: New York; 2001.
[36] L. Pishkar, M. Monajjemi, A. R. Ilkhani, F. Mollaamin, International Journal of the Physical Sciences 5 (2010) 1450.
[37] F. Mollaamin, K. Shahani poor, T. Nejadsattari, M. Monajjemi, African Journal of Microbiology Research, 4 (2010) 2098.